NASA TT F-9870

PRESENT POSSIBILITIES FOR A THEORETICAL STUDY OF A SUPERSONIC EJECTOR NOZZLE

Jean-Marie Hardy and Jean Delery

Translation of "Possibilités actuelles d'étude théorique d'une tuyère supersonique à double flux".
Paper presented at A.G.A.R.D. Specialists Meeting on the Aerodynamics of Power Plant Installation, A.E.D.C., Tullahoma, October 25-28, 1965. Reprint #288.

NATIONAL AERONAUTICS AND SPACE ADMINISTRATION
WASHINGTON JANUARY 1966

1657

At high secondary mass flow rate, the two streams of the ejector retain their individuality, requiring calculation of the primary jet by the method of characteristics and of the secondary stream by the hypothesis of a one-dimensional flow. A corrective term is derived for taking the mass flow, entrained by viscous mixing along the nonisobaric interface of the two streams, into consideration. Performance curves, calculation schemes, and flow patterns are given for angular criteria of re-attachment of flow, boundary-layer effects, momentum, pressure distribution along the divergent section, and entrainment effects due to mixing.

Author

NATIONAL AEROSPACE RESEARCH AND DEVELOPMENT ADMINISTRATION
29, Avenue de la Division Leclerc Chatillon-sous-Bagneux (Seine)

PRESENT POSSIBILITIES FOR A THEORETICAL STUDY OF A SUPERSONIC EJECTOR NOZZLE

Jean-Marie Hardy and Jean Delery

Paper presented at the AGARD Specialists Meeting on the Aerodynamics of Power Plant Installation, Tullahoma, October 25 - 28, 1965

PRESENT POSSIBILITIES FOR A THEORETICAL STUDY OF A SUPERSONIC EJECTOR NOZZLE

*/1

Jean-Marie Hardy and Jean Delery

16577

A brief review is given over the methods used in computing supersonic ejector nozzles with low and high secondary mass flow rates. Empirical data are given for demonstrating the excellent agreement for cases in which the fluid used for the primary and secondary streams is air at ambient temperature. For the case of a real air exit (variable γ and temperature), a critical review over the theory demonstrates that the influence of these factors is taken into consideration in cases of high mass flow rate.

Author

1. Introduction

/2

The design and construction of supersonic transports requires a thorough study of the propulsion unit.

The great variety of flight regimes, encountered during a given mission, raises difficult adaptation problems for the constituent elements of the unit, namely, air intake, turbojet engine, and ejector nozzle.

Specifically, the design of such an ejector involves a highly complex internal aerodynamics problem. The nozzle is subject to widely differing operating conditions, with the expansion rate varying from 2 on takeoff and landing to values between 15 and 20 at supersonic cruising. In addition, modern turbomachines require an accurate regulation of their air throughput.

---

* Numbers in the margin indicate pagination in the original foreign text.

These requirements can be satisfied by a nozzle with variable throat cross section and divergence angle. However, the resultant technological complication makes this approach to the problem difficult to realize at the present state of the art.

Therefore, nozzles with multiple streams are preferred at present, in which the adaptation to the various operating regimes is obtained by aerodynamic means.

This solution increases the technological simplicity and, without a noticeable increase in external drag, has the advantage of permitting the removal of air discharges at low base pressure, coming from boundary-layer bleeds of the air intake, from cooling circuits, and possibly from the mass flows of a "by-pass" of the airscoop.

Figure 1 gives a schematic sketch of the arrangement of a double-stream nozzle. This ejector comprises a sonic throat of variable cross section A_c, through which emerges the primary stream whose base pressure and temperature are high. This flux expands in a divergent portion whose minimum cross section A is greater than A_c, entraining the secondary stream whose base pressure and temperature levels are much lower than those of the main flow.

A determination of the performance of thrust and discharge of such a device, whose operating principle is similar to that of a supersonic ejector, is made highly complex by the large number of parameters involved. For this reason, an optimum solution will require numerous and costly experiments and tests.

Therefore, it is of considerable interest to develop calculation methods for predicting the performance of an ejector of this type with sufficient accuracy to reduce the developmental tests to a minimum.

The work done during the past years, in France as well as in the United

States, has considerably advanced the theory of supersonic ejectors. Because of the data acquired in this manner, the ONERA (National Aerospace Research and Development Administration) and the SNECMA (National Company of Research and Construction of Aircraft Engines), working in close collaboration, have developed computation methods that, in a satisfactory manner, permit predicting the performance of a given ejector over the entire extent of its operating domain. /3 These methods are programed on large electronic computers of the IBM 704 and IBM 7040 type, and are now in the course of exploitation.

After a brief description of the phenomena of the internal aerodynamics of an ejector, we will discuss first the case of weak and then of strong secondary streams. These two variants correspond to distinct flow patterns and thus require different computational methods, whose applicability will be discussed on the basis of a comparison with empirical data.

2. Phenomenology; Various Operating Regimes of an Ejector

In a cruising flight, two different types of operation may be encountered, corresponding to distinctly differing primary and secondary flow patterns.

If the mass flow of the secondary stream is weak or zero, the primary stream will expand, at the exit from the ejector nozzle, in the form of an isobaric free jet. This jet becomes re-attached to the wall of the divergent section of the return, undergoing a rapid recompression which leads to a focalization shock or Mach wave (see Fig.2).

The secondary injection cavity or sink encloses a region of low-velocity fluid at constant pressure, known as "dead water". Along the interface, separating this dead-water zone from the supersonic jet, the turbulent viscosity phenomenon results in the development of a mixing zone, which is the site of

energy and mass exchanges that permit the primary stream, by viscous entrainment, to remove a certain amount of secondary mass flow.

The pressure distribution over the wall of the divergent section (see Fig.2) is characterized by an isobaric zone followed by a rapid recompression in the region of re-attachment of the primary jet. Downstream of this region, the pressure evolution corresponds to the expansion of the flow, re-attached along the divergent section.

If the secondary mass flow is large, the two streams will retain their individuality and remain separate on either side of a fluid boundary along which a nonisobaric mixing layer develops (see Fig.3).

The secondary stream, injected at low velocity, is progressively accelerated in the convergent interval which is established along the fluid boundary and the wall of the divergent interval. For a sufficiently elevated injection pressure, sonic velocity is reached in the minimum passage cross section available to the secondary stream.

The pressure distribution along the wall of the divergent section now presents a continuously increasing slope, analogous to that observed in the classical divergent nozzle (see Fig.3).

Each of these two operating regimes corresponds to a specific computation method which will be discussed below for either of the two cases.

3. Nozzle Performance Calculation for Low Secondary Mass Flow Rate /4

The calculation of the ejection performance, in the case of low secondary mass flow rates, is based on the results of theoretical work concerning the problem of turbulent re-attachment of flow. This includes work done in the United States by H.H.Korst (Bibl.1) and in France at the ONERA by P.Carrière

and M.Sirieix (Bibl.2, 3).

First, we will briefly review the basic points of the theory of turbulent re-attachment of flow, described in the reports by the above authors.

3.1 Theory of Turbulent Re-Attachment

This theory, which was originally established for a uniform supersonic two-dimensional flow, can be extended also to nonuniform flows if the thickness of the mixing zone is small relative to the length of the isobaric boundary of the primary jet.

In this case, the conditions prevailing at the boundary of the viscous zone are related to those established at the isobaric limit of the jet assumed to be nonviscous.

The theory of re-attachment, in the form in which it is presented elsewhere (Bibl.2), postulates the existence of a functional relation between the deviation Ψ suffered by the flow at the level of re-attachment and the conditions characterizing the state of the flow directly upstream of the recompression zone, along the streamline osculating the point of re-attachment and known as border line.

This relation which is denoted as the angular re-attachment criterion, has the form

$$\Psi = \Psi (M_1 , \pi_{i\ell})$$

where M_1 is the Mach number at the isobaric boundary of the jet, while p_{i_ℓ} is the base pressure along the border line.

To determine the conditions on the border line, the theory of turbulent mixing is used. This theory indicates that, in the absence of an initial boundary layer, the velocity profiles throughout the mixing zone exhibit the

property of similitude. Making use of the reduced variable $\eta = \sigma \frac{y}{s}$, where σ is a mixing parameter and y and s are intrinsic coordinates of the moving point, the velocity profiles can be approximately represented by the function

$$\varphi = \frac{u}{u_1} = \frac{1}{2}\left(1 + \operatorname{erf} \eta\right) \tag{1}$$

The profiles are staggered in accordance with y, relative to the boundary of the nonviscous flow, in such a manner that, at each abscissa, the law of the conservation of momentum is obeyed.

The border line (see Fig.4) is defined by its reduced ordinate η_ℓ which, in turn, can be determined by writing the relations of the laws of the conservation of mass.

Denoting by q the mass flow entering the dead-water zone per unit enclosure, by i the momentum supplied by this injection, and by δ^{**} the thickness of momentum of the initial boundary layer, then the laws of conservation permit calculating η_ℓ, at the abscissa s, by means of the relation

/5

$$\int_{-\infty}^{\eta_\ell} \frac{\rho}{\rho_1} \varphi \, d\eta = \frac{\sigma}{\delta}\left(\frac{q}{\rho_1 u_1} - \frac{i}{\rho_1 u_1^2} - \delta^{**}\right) + \int_{-\infty}^{+\infty} \frac{\rho}{\rho_1} \varphi (1-\varphi) \, d\eta. \tag{2}$$

Carrière (Bibl.3) defined a generalized injection coefficient, by posing

$$C_q = \frac{q}{\rho_1 u_1 s} - \frac{i}{\rho_1 u_1^2 s} - \frac{\delta^{**}}{s}. \tag{3}$$

If q, i, and δ^{**} are moderate, their influence on the shape of the velocity profiles is negligible. These profiles can then be represented, to within one translation, by eq.(1) which, in principle, is uniquely valid for an isobaric mixing zone without initial boundary layer and at zero velocity in the dead water or wake.

If, in addition, we postulate a hypothesis on the law of evolution, as a

function of φ, of the total temperature throughout the mixing zone (turbulent Prandtl number equal to 1), then eq.(2) can be solved so that η_ℓ can be calculated. The result has the following form:

$$\eta_\ell = \eta_\ell \left(M_1 , \frac{T_{is}}{T_{ij}} , \gamma , C_q \right) , \tag{4}$$

where T_{ij} denotes the base temperature of the primary supersonic flow, while T_{is} is the temperature of the wake.

Taking eqs.(1) and (4) into consideration, the angular re-attachment criterion is written as

$$\Psi = \Psi \left(M_1 , \frac{T_{is}}{T_{ij}} , \gamma , C_q \right) . \tag{5}$$

If C_q is sufficiently small, which generally is the case, eq.(5) can be written in the following linearized form:

$$\Psi = \Psi_o \left(M_1 , \frac{T_{is}}{T_{ij}} , \gamma \right) + \lambda \left(M_1 , \frac{T_{is}}{T_{ij}} , \gamma \right) C_q . \tag{6}$$

In this form, the angle of re-attachment Ψ_o is obtained, corresponding to the nonperturbed ideal case, i.e., in the absence of any mass injection effect or boundary layer; the relation also furnishes the gradient $\lambda = \partial\Psi/\partial C_q$ which characterizes the mass injection effect and the perturbing effects of the momentum and the initial boundary layer.

The functions Ψ_o and λ are readily obtained by making use of the criterion proposed by H.H.Korst and D.R.Chapman. This criterion postulates that the generating pressure along the border line, at the instant at which this line approaches the re-attachment point, must be equal to the static pressure after re-attachment. This condition is directly obtained in the form of an angular relation

/6

$$\Psi = \Psi \left(M_1 , \varphi_\ell \right) .$$

However, practical experience has demonstrated that the use of this criterion leads to secondary pressure levels that are distinctly higher than the measured values. Conversely, the relative pressure variation, due to an injection effect, is accurately predicted.

Returning to eq.(6), it seems that the law of re-attachment at zero blast, obtained from the Chapman-Korst criterion, is incorrect.

Under these conditions it is preferable to use practical experiments for defining an empirical law of re-attachment Ψ_0 which, when substituted for the theoretical law, eliminates the quantitative discrepancy of the theory.

A basic study conducted at the ONERA (Bibl.5) made it possible to establish such a law for the case of a jet of revolution, becoming re-attached to a coaxial cylindrical wall with a configuration close to that of an ejector because of the low aperture angle of conventional divergent sections.

The resultant law of angles, which corresponds to the case $\frac{T_{i_s}}{T_{i_j}} = 1$ and $\gamma = 1.4$, is plotted in Fig.5. The diagram also gives the evolution of Ψ_0, derived from the Chapman-Korst criterion. There is a considerable deviation between the two curves, corresponding to a fictive mass injection effect, characterized by a practically constant C_q equal to 0.005. Therefore, in practical application, one can use the Chapman-Korst criterion and then correct the obtained values of C_q by adding 0.005.

This correction, rigorously valid for $\gamma = 1.4$ and $T_{i_s}/T_{i_j} = 1$, represents only an approximation when the state and type of the gases used result in different values of these parameters, because of the lack of sufficiently accurate and extensive empirical data.

When this is the case, then the relation

$$\Psi = \Psi_0 \left(M_1, \frac{T_{is}}{T_{ij}}, \gamma \right) + \lambda \left(M_1, \frac{T_{is}}{T_{ij}}, \gamma \right) \cdot \left(C_q - 0.005 \right), \qquad (6')$$

where Ψ_0 and λ were calculated according to the discharge hypothesis by Korst, together with the equation expressing the conservation of energy in the wake

$$R = R \left(\frac{T_{is}}{T_{ij}}, C_q \right) \qquad (7)$$

permit a complete solution of the problem of re-attachment (determination of C_q and T_{i_s}/T_{i_j} for a given M_1).

Hovever, at the present state of the art, these relations merely are an approximation and only permit an estimate of the qualitative effects due to various influence factors. /7

3.2 Practical Method of Calculation; Comparison with Experiment

The calculation of thrust and discharge of an ejector is performed in two steps.

In the first step, the nonviscous primary supersonic flow is computed. This calculation permits determining the shape of the isobaric boundary of the free jet as well as the pressure distribution along the wall of the divergent section, from which the nozzle thrust coefficient can be derived.

The supersonic flow is calculated by the method of characteristics. This calculation includes the determination of the shock wave, shed from the re-attachment point. The initial data comprise: the last characteristic of the actual influence domain of the primary nozzle, the secondary pressure level, and the geometry of the divergent section. This computation was programed on IBM 704 and IBM 7040 computers. The computation allows for the variations in the specific heat ratio as a function of the temperature and for the composition

of the air-kerosene combustion gases. Figure 6, as a typical example, gives the characteristic curves obtained for a nozzle with a conical divergent section and a ratio of p_{i_s}/p_{i_j} equal to 0.131.

In the second step of the calculation, the viscosity effects are superimposed on the ideal gas flow. This permits determining the secondary mass flow, entrained by the primary jet. The calculation is based on considerations developed in the preceding Section.

If the isobaric boundary of the nonviscous jet is known, the border line can be localized by calculating its reduced ordinate η_ℓ. The intersection of the border line with the wall is the point of theoretical re-attachment. This point is projected onto the boundary (f) of the nonviscous jet, in accordance with the mean normal to the two curves (see Fig.4). The local direction of the velocity in the undisturbed flow directly yields the value of the angle of re-attachment Ψ.

If the two existing streams are of the same type and have the same base temperatures, eq.(6) will permit calculating the generalized injection coefficient C_q which, after correction for the effects of the initial boundary layer and the momentum, yields the injection coefficient $q/e_1\mu_1 s$ where s is the length of the isobaric boundary comprised between the separation point and the re-attachment point R [this calculation method is explained elsewhere (Bibl.6)].

Figure 7 gives a comparison of theoretical and experimental results on the discharge performance at low secondary flow rate, for a cylindrical ejector with a slightly conical primary nozzle (exit Mach number, close to 1.4). The fluid used is air at ambient temperature (case of T_{i_s}/T_{i_j}, $\gamma = 1.4$).

The calculation of the entrained mass flow was performed by using the /8 empirical law of re-attachment shown in Fig.5. Allowance has been made for the

effects of the initial boundary layer and of the momentum.

These results show satisfactory agreement between the modified theory and practical experiments for injection rates as high as 0.04, which closely corresponds to the limit of discharge potentiality by isobaric mixing. For higher injection rates, the primary jet no longer re-attaches to the wall of the divergent section, and the second operating regime in which the two streams maintain their individuality will become established.

The curves plotted in Fig.8 demonstrate, as a typical example, the influence on the theoretical results when allowing for the effects of the initial boundary layer and of the momentum. The significance of the initial boundary layer effect is especially high when the injection rate is low; the diagram also shows the increasing influence of the effect of momentum when the secondary mass flow rate increases.

The use of the generalized injection coefficient C_q, defined in Section 3.1, makes it possible to allow for these effects in a simple and highly accurate manner, at least so long as these effects are moderate.

3.3 Pressure Distribution along the Wall of the Divergent Section and Thrust Coefficient

The calculation of the flow in a perfect fluid, using the method of characteristics, leads to a pressure distribution along the wall of the divergent section, presenting a discontinuity at the point of impact of the isobaric boundary of the jet.

In fact, this calculation assumes that the recompression of the primary flow, at the level of re-attachment, takes place over an attached oblique shock wave. In reality, this recompression is progressive, and the line of the jet

is isobaric only over a fraction of its theoretical length.

Figure 9 gives a comparison between the theoretical and experimental distributions, for the case of a cylindrical return wall.

Except in the zone of re-attachment, the theoretical curve agrees well with practical experiments, and in the case of diverging nozzles the error committed in evaluating the thrust coefficient from the calculated distributions is minimal.

4. Nozzle Performance Calculation for High Secondary Mass Flow Rate

Assuming that the base conditions of the primary stream and the geometry of the double-stream nozzle are known, it is desired to determine the discharge performance and the thrust coefficient for the case - generally present in cruising flight of a supersonic transport - in which the secondary flow is blocked because of the fact that sonic velocity has been reached in a certain portion of the divergent part.

4.1 Model of the Calculus Used /9

As a general rule, when the secondary mass flow rate of a fully started ejector, operating in the supersonic regime, is sufficiently large, the phenomena of viscous interaction are limited to a narrow region which, on the one hand, comprises the boundary layer established at the wall of the divergent section and, on the other hand, the nonisobaric mixing zone that develops at the interface of the two flows.

Since both are subject to the favorable influence of a negative pressure gradient, these "viscous layers" are relatively thin so that it is logical, in first approximation, to neglect their effect; each of the two streams then main-

tains its individuality and obeys the laws of flow of nonviscous perfect fluids.

From this viewpoint, a simplified calculation model has been proposed independently by P.Carrière (Bibl.7) and by H.H.Korst, W.L.Chow, and A.L.Addy (Bibl.8, 9). This model is based on the following simplifying hypotheses, substantiated by practical experiments:

The mixing layer is assimilated at a velocity discontinuity surface, on either side of which the pressures are equal.

The secondary stream is one-dimensional and isentropic; this stream behaves as a sectional flow, each section constituting the area comprised between the moving point (d) of the common interface (f) and the wall of the divergent section, normal to the mean direction (see Fig.10).

The supersonic primary stream (1) can be defined by the method of characteristics, since the pressure prevailing at (d) and equal to that of the secondary stream (2) is imposed by the condition of coexistence of the two flows in the divergent section.

The calculation procedure is described below, taking as example the classical double-stream device shown in Fig.10, operating at an expansion rate such that the flow (1) is entirely supersonic in the divergent section.

For a given value p_{0_s} of the secondary inlet pressure, let us define a secondary Mach number M_{0_s}. This reduces to fixing a value for the secondary stream, which we will characterize by the coefficient $\mu = \frac{Q_s}{Q_j}\sqrt{\frac{T_{i_s}}{T_{i_j}}}$.

The expansion of the primary flow in C is determined by the condition of pressure equality $p_{0_j} = p_{0_s}$ directly downstream of C. From this, the network of drooping characteristics (ξ), forming the expansion surface issuing from C, can be constructed.

Determination of the point (d), infinitely close to C along the interface (f) of the two flows, is obtained in the following manner: The intersection of the tangent to (f) in C, with the rising characteristic emerging from (c') close to C on the last characteristic of the expansion surface, will yield a first approximation (d').

Knowing (d'), the area A_{1_s} available to the secondary stream can be derived, yielding the ratio /10

$$\frac{A_{1s}}{A_{0s}} = \frac{\Sigma(M_{1s})}{\Sigma(M_{0s})}$$

which defines the secondary Mach number M_{1_s} as well as $p_{i_s} = p_{i_j}$ in (d').

The characteristic relation, written between (c') and (d'), will then permit determining the direction of the velocity in (d').

The calculation is resumed this time by comparing the interface (f), not to its tangent in C, but to a straight line whose direction is the mean between those of the tangents in C and (d'). This process is repeated until the results converge.

Knowing (d), the characteristic (ξ_d) is determined step by step; again using the above method, the quantity (d') and thus also the complete definition of (f) will be obtained.

If the ejector has not been started, the evolution of the secondary flow will be entirely subsonic in the divergent section, since the Mach number at the exit reaches a maximum value of less than 1. In this case, the calculation presents no difficulty.

However, it should be mentioned that the corresponding regime is physically acceptable only if the pressure reached by the secondary flow at the exit is equal to the ambient pressure.

In the practical cases considered here, this possibility is excluded.

Investigations on the supersonic regime of the ejector at p_{0_s} are conducted by successive tests. A priori, decreasing values of the Mach number M_{0_s} are selected until the blocking conditions are satisfied, i.e., until the cross section where the secondary flow becomes sonic coincides with the minimum cross section offered to the secondary stream by the primary flow.

The method to be described below requires high-capacity electronic computers for its practical application.

The programing was made on an IBM 7040 computer by the SNECMA (Bibl.10), with the following simplifications:

a) The Mach number M_{0_s}, corresponding to the critical conditions, is determined as soon as the difference between two successive iterations is below 10^{-3}.

b) In the region in which the induced stream is transonic ($0.95 < M < 1.05$), the cross section available to the secondary stream is practically stationary. The pressure condition is then replaced by a wall condition at the boundary of the primary jet, obtained by assuming that the primary stream is flowing within a fictive nozzle whose cross section, in a given plane, is equal to the cross section of the ejector, reduced by the a priori fixed secondary critical /11 cross section. The local development of the pressure p of the primary stream in this domain furnishes the Mach number distribution of the secondary flow, from the following isentropic relation:

$$M_s = f\,(p/p_{i_s}).$$

Figure 11, as a typical example, gives the pattern of the flow in-

side a nozzle with conical divergent section, for a secondary injection rate $\mu = \frac{Q_s}{Q_j}\sqrt{\frac{T_{i_s}}{T_{i_j}}}$ equal to 0.07.

4.2 Effect of Entrainment due to Mixing

In a general manner, the turbulent mixing produced at the interface of the two streams leads to a displacement of the streamline separating these two streams, relative to the nonviscous theoretical boundary. The loss in momentum, suffered by the flow (1), leads to a gain of the same extent for the stream (2).

This shift or displacement is negligible so long as the thickness of the mixing zone is small with respect to the transverse extent of the two streams (which is the case when μ is higher than 0.1).

Conversely, as soon as μ diminishes, the entrainment effect of the secondary stream by the primary flow must be taken into consideration.

The method suggested by W.L.Chow and A.L.Addy gives a satisfactory solution of this problem and has the additional advantage of entering only in the form of a correction to be made on the results obtained by assuming nonviscous fluids.

Making use of simplified solutions of the equations of motion, derived for the case of an isobaric mixing of the two flows having different velocities u_1 and u_2 ($u_1 > u_2$), the above authors - by analogy with the treatment of boundary layers - define a "displacement thickness" δ^* which represents the effect of entrainment.

The quantity δ^* is calculated in reduced variables and can be represented by a relation of the form

$$\frac{\sigma\,\delta^*}{s} = f\left(M_1, \gamma, \frac{T_{i_2}}{T_{i_1}}, \frac{u_1}{u_2}\right). \qquad (8)$$

In this expression, σ is a mixing parameter, given by a semi-empirical relation of the type of

$$\sigma = \sigma \left(M_1 , \gamma , \frac{\mu_2}{\mu_1} \right).$$

Equation (8), applied to the critical point ($M_{c_s} = 1$) and calculated for a perfect fluid, leads to a corrective term for the entrained mass flow, which is expressed in the form of

$$\frac{\Delta Q_s}{Q_s} = - \frac{2\pi R \delta^*}{A_{c_s}} ,$$

where R is a mean value of the distance between the axis and the mixing zone, /12 at the level of the critical cross section.

The curves of theoretical discharge performance, plotted in Fig.12, indicate the significance of allowing for viscosity effects. It will be found that the relative error, committed by neglecting the mass flow entrained by the viscous mixing, is always small and becomes practically negligible as soon as μ exceeds 10%.

Under these conditions, it is likely that the calculation of gaseous flows whose type and temperature differ greatly presents no major difficulty, since the effects due to turbulent transport are rather insignificant and can be roughly estimated.

4.3 Comparison of Theoretical Results with Experiments

Numerous experiments, made with the purpose of defining the ejector of a supersonic transport, have made it possible to test the validity of the various theoretical methods developed. As an illustrative example, we will discuss some of the comparisons of theory and experiment, obtained from these tests. All results given here correspond to the case $T_{t_j} = T_{t_s}$, $\gamma = 1.4$. Later in the

text, we will give a brief summary of the influence of any variation in γ.

Figure 13 gives a comparison between the pressure distributions at the wall of the divergent section, obtained by calculation and experiment. The geometry of the ejector is schematically sketched in the upper portion of the diagram. This arrangement comprises a primary ejector with a sonic throat and a truncated-cone return wall, having a divergence angle of 9.5°. The ratio of the throat cross section to the initial cross section of the divergent portion is 1.8.

The pressure distributions are represented by two different values of the secondary injection rate: in one case, $\mu = 0.05$ and, in the other case, $\mu = 0.1$ both of which represent measured values; the calculated values are equal to 0.046 and 0.103, respectively.

The agreement between theory and experiment can be considered highly satisfactory. The computational program developed here - as proved by these results - covers entirely arbitrary shapes of the divergent section, including abrupt and extensive cross-sectional variations.

Figure 14 gives a comparison of theory and experiment, with respect to the overall performance of an ejector of this type. Figure 14a gives the development of the thrust coefficient C_T as a function of the secondary injection rate. The thrust coefficient is defined as the ratio of the gross thrust of the nozzle to the ideal gross thrust of the primary jet; this ideal thrust was calculated by assuming that the primary jet expands isentropically from a base pressure p_1, to a pressure at infinity downstream p_∞.

It can be stated that the agreement between theory and experiment is /13 excellent for injection rates μ above 0.02. For rates less than this value, the agreement is less good. The apparently anomalous slope of the theoretical curve probably can be attributed to the fact that the re-attachment of the pri-

mary jet takes place at the level of the wall discontinuity, defining the extremity of the secondary injection bleed.

An investigation of this specific case will be the subject matter of a later publication.

Figure 14b represents the discharge performance curve of the nozzle. The ordinate gives the ratio of the secondary base pressure to the base pressure of the primary jet. The agreement between theory and experiment can be considered satisfactory for values of μ above 0.02. For values of μ below 0.02, the theoretical curve, for the same reason, shows the same anomalous slope as the curve for the thrust coefficient.

4.4 Influence of γ on the Theoretical Performance of an Ejector

In practical application, the primary jet usually consists of air-kerosene combustion gases. Because of their high base temperature and their chemical composition, these gases have a specific heat ratio differing from 1.4. Therefore, it is important to define the influence of γ on the performance of an ejector, if the results from wind-tunnel tests, which usually are performed with air of a temperature close to the ambient, are to be extrapolated to real conditions.

Figure 15 shows the influence of γ on the thrust and discharge performance of an ejector. The curves were calculated for two values of γ_j, namely, 1.4 and 1.335. In a general manner, for the same secondary injection rate, the thrust coefficient and the secondary base pressure are higher the lower the ratio of specific heat of the primary jet becomes. This effect is primarily due to the influence of γ on the configuration of the boundary of the primary jet. In fact, other conditions being equal, the volume occupied by the primary

jet increases with decreasing γ. Because of this, the cross section of the passage available to the secondary stream is restricted, so that also the discharge rate will reduce. Consequently, if equal discharge rate is to be maintained, the secondary base pressure must be increased. This will lead to a general rise of the pressure level at the wall of the divergent section, leading to an increase in the nozzle thrust coefficient.

5. Conclusions

Recent progress made in the theory of supersonic ejectors will permit an accurate prediction of the performance of thrust and discharge of double-stream nozzles in their entire operating domain.

If the secondary mass flow is low ($\mu < 0.04$), the primary jet will become re-attached to the wall of the return passage. The discharge of the secondary stream then takes place exclusively by viscous entrainment along the isobaric boundary of the primary flow. In this case, the calculation of the exit mass flow rate will have to be based on the turbulent re-attachment theory developed by H.H.Korst, modified by the introduction of an empirical law of re-attachment. The use of a generalized discharge coefficient also permits allowing for the /14 effect of the momentum produced by the secondary injection, as well as for the effect of the initial boundary layer of the primary jet.

If the secondary mass flow rate is high, the two streams will retain their individuality. The flows are then calculated by assuming perfect fluids: The primary jet is determined by the method of characteristics, and the secondary stream is calculated on the hypothesis of a one-dimensional flow.

The uniqueness of the solution is ensured by the condition of blocking of the secondary flow. A corrective term is then estimated, by which the mass

flow, entrained by viscous mixing along the nonisobaric interface of the two flows, can be taken into consideration.

The agreement between theoretical and experimental results can be considered absolutely satisfactory in the case in which the two flows are constituted by air, at a base temperature close to the ambient value.

With respect to the influence of the temperature and the type of gas, the following statements can be made:

In the case of low secondary mass flow rates, the theoretical scheme proposed by Korst can be considered as being qualitatively valid, permitting an estimate of the variations in secondary base pressure due to the effects of injection and initial boundary layer. However, the lack of accurate data as to the influence of γ and of the temperature on the empirical law of re-attachment, introduced for correcting Korst's theory, does not yet permit an absolute assurance that the estimate of the secondary pressure levels is quantitatively correct. The ONERA has scheduled a study of this particular subject.

In the case of high secondary mass flow rates, the influence of these factors on the development of the mixing zone, separating the two streams, is relatively insignificant in making estimates of the nozzle performance. Such an estimate can be made, without the risk of excessive errors, by using the method suggested elsewhere (Bibl.8). The basic principle of these effects must be taken into consideration in any calculation based on perfect fluids; this presents no difficulty for the usually encountered temperature levels.

NOTATIONS /15

Symbols

M = Mach number

p = pressure

ρ = specific mass

T = absolute temperature

γ = ratio of specific heats

u = longitudinal velocity component

q = unit mass flow (per unit enclosure)

Q = mass flow rate

μ = secondary injection rate $\mu = \frac{Q_s}{Q_j}\sqrt{\frac{T_{i_s}}{T_{i_j}}}$

i = momentum

δ^{**} = momentum thickness of the initial boundary layer

φ = reduced velocity: $\varphi = \frac{u}{u_l}$

C_q = generalized injection coefficient

σ = mixing parameter

y, s = intrinsic coordinates fixed with respect to the velocity profile

η = reduced ordinate: $\eta = \sigma \frac{y}{s}$

Ψ = re-attachment angle

Σ = isentropic cross-sectional ratio: $\Sigma = \frac{A}{A_c}$

Subscripts

i = base conditions

l = conditions at the boundary of the supersonic jet

s = secondary flow

j = primary jet

c = critical conditions

ℓ = conditions along the border line

BIBLIOGRAPHY /16

1. Korst, H.H., Page, R.H., and Childs, M.E.: A Theory for Base Pressure in Transonic and Supersonic Flow. ME-TN - 392 - 2. University of Illinois, 1955.

2. Carrière, P. and Sirieix, M.: Influence Factors of the Re-Attachment of a Supersonic Flow (Facteurs d'influence du recollement d'un écoulement supersonique). Congrés de Mécanique Appliquée, STRESA, 1960, and Publication ONERA, No.102, 1961.

3. Carrière, P.: Recent Research on the Problem of Base Pressure (Recherches récentes sur le problème de la pression de culot). ONERA - T.P., No.18, 1963.

4. Carrière, P. and Sirieix, M.: Recent Results of Investigations on the Mixing and Re-Attachment Problems (Résultats récents dans l'étude des problèmes de mélange et de recollement). Congrès de Mécanique Appliquée, Munich, 1964.

5. Delery, J.: Re-Attachment of a Supersonic Jet of Revolution on a Coaxial Cylindrical Wall (Recollement d'un jet supersonique de révolution sur une paroi cylindrique coaxiale). La Recherche Aérospatiale, No.104, January-February 1965.

6. Sirieix, M.: Contribution to the Study of Supersonic Ejectors (Contribution à l'étude des éjecteurs supersoniques). Association Technique Maritime et Aéronautique, Session 1963.

7. Carrière, P.: Calculation of Turbulent Mixing of Two Heterogeneous Flows /17 in an Ejector (Calcul du mélange turbulent de deux écoulements hétérogènes dans un éjecteur). ONERA In-House Tech. Note, April 1962.

8. Chow, W.L. and Addy, A.L.: Interaction between Primary and Secondary Streams of Supersonic Ejector Systems and their Performance Characteristics. AIAA Journal, Vol.2, No.4, April 1964.

9. Addy, A.L.: On the Steady State and Transient Operating Characteristics of Long Cylindrical Shroud Supersonic Ejectors (with Emphasis on the Viscous Interaction between the Primary and Secondary Streams). Ph.D. Thesis, Dept. of Mechanical Engineering, Univ. of Illinois, June 1963.

10. Lacombe, H.: Calculation Method for Ejectors (Méthode de calcul des éjecteurs). SNECMA In-House Report (to be published).

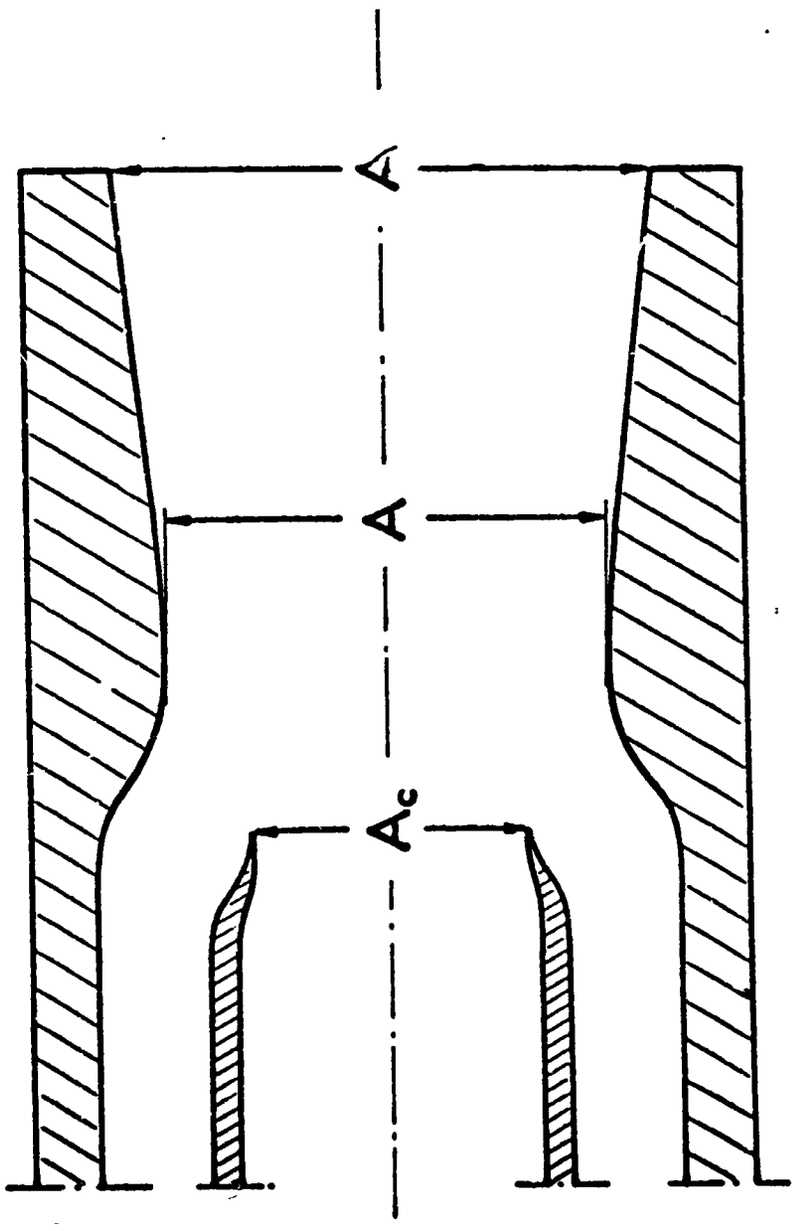

Fig.1 Sketch of a Supersonic Ejector

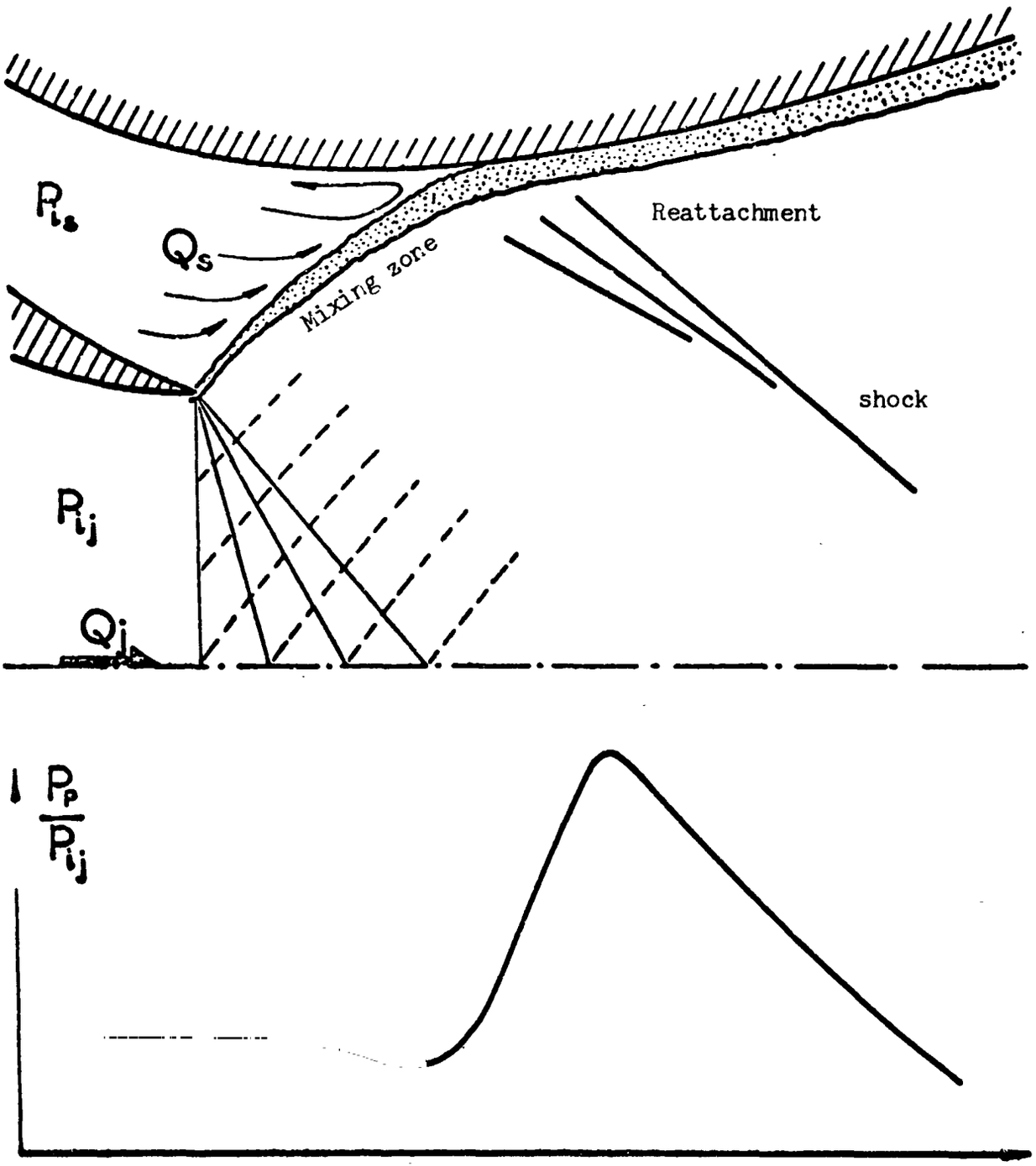

Fig.2 Low Secondary Mass Rate of Flow

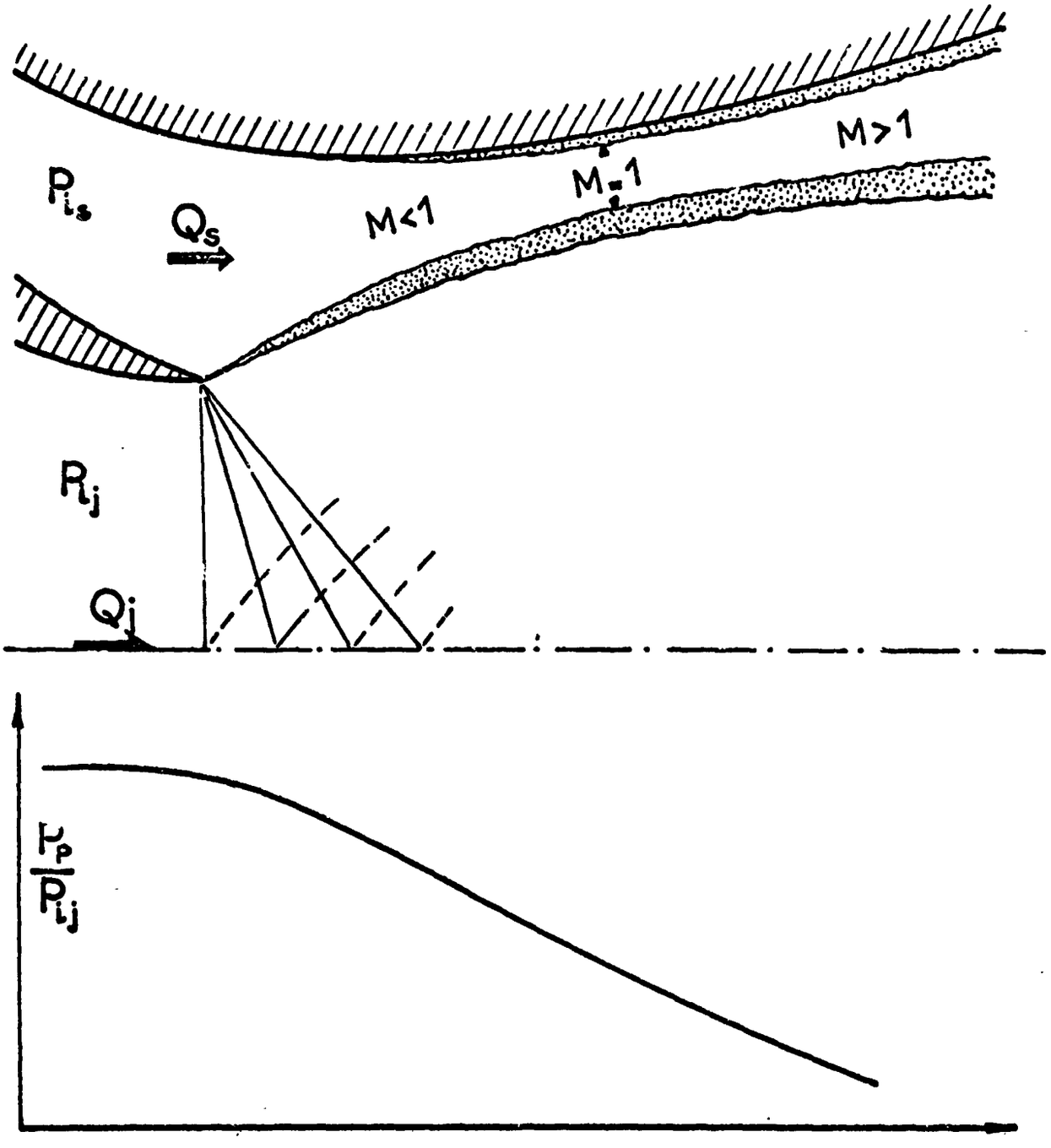

Fig.3 High Secondary Mass Rate of Flow

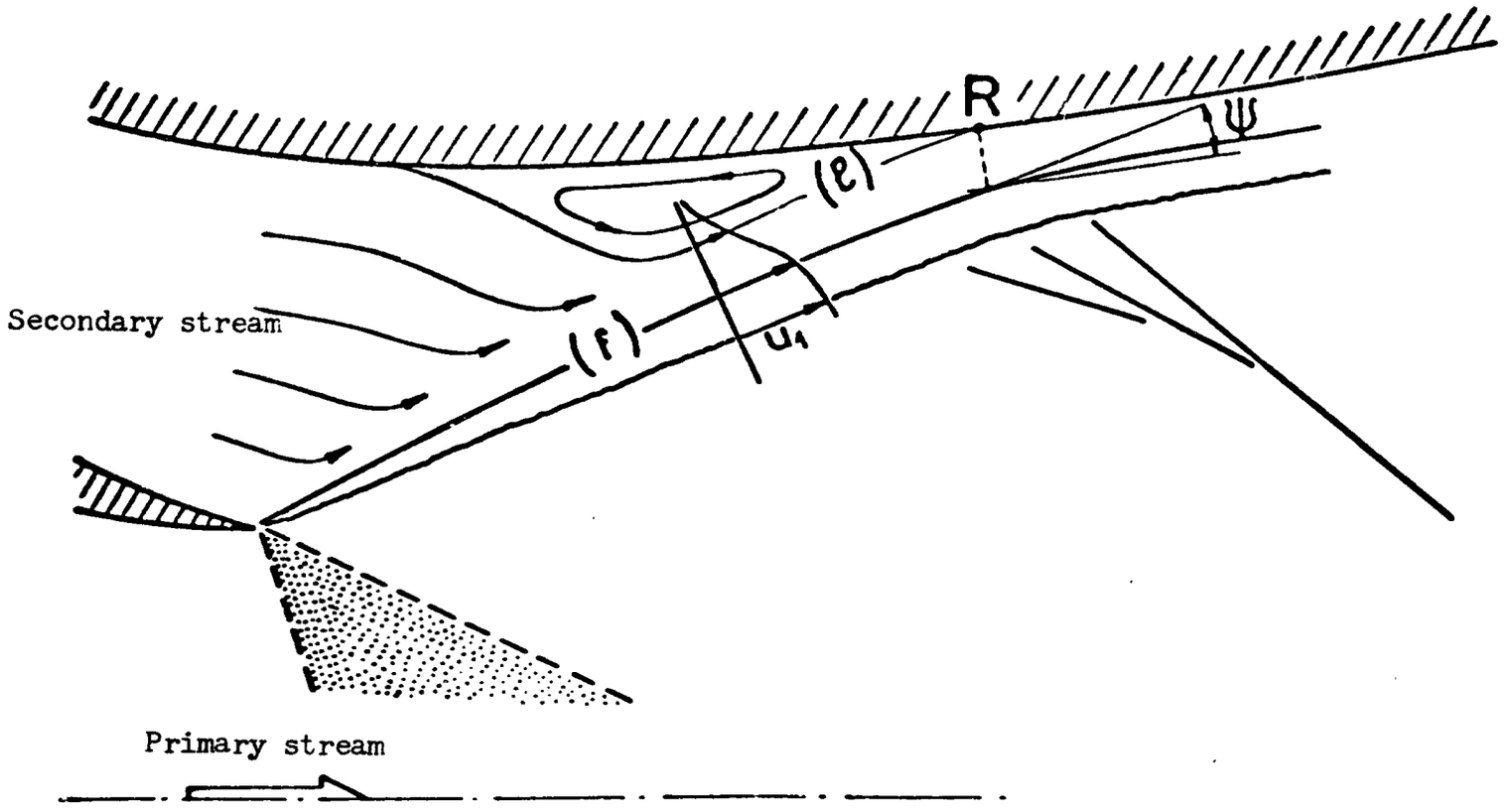

Fig.4 Theoretical Schematic Diagram of Re-Attachment

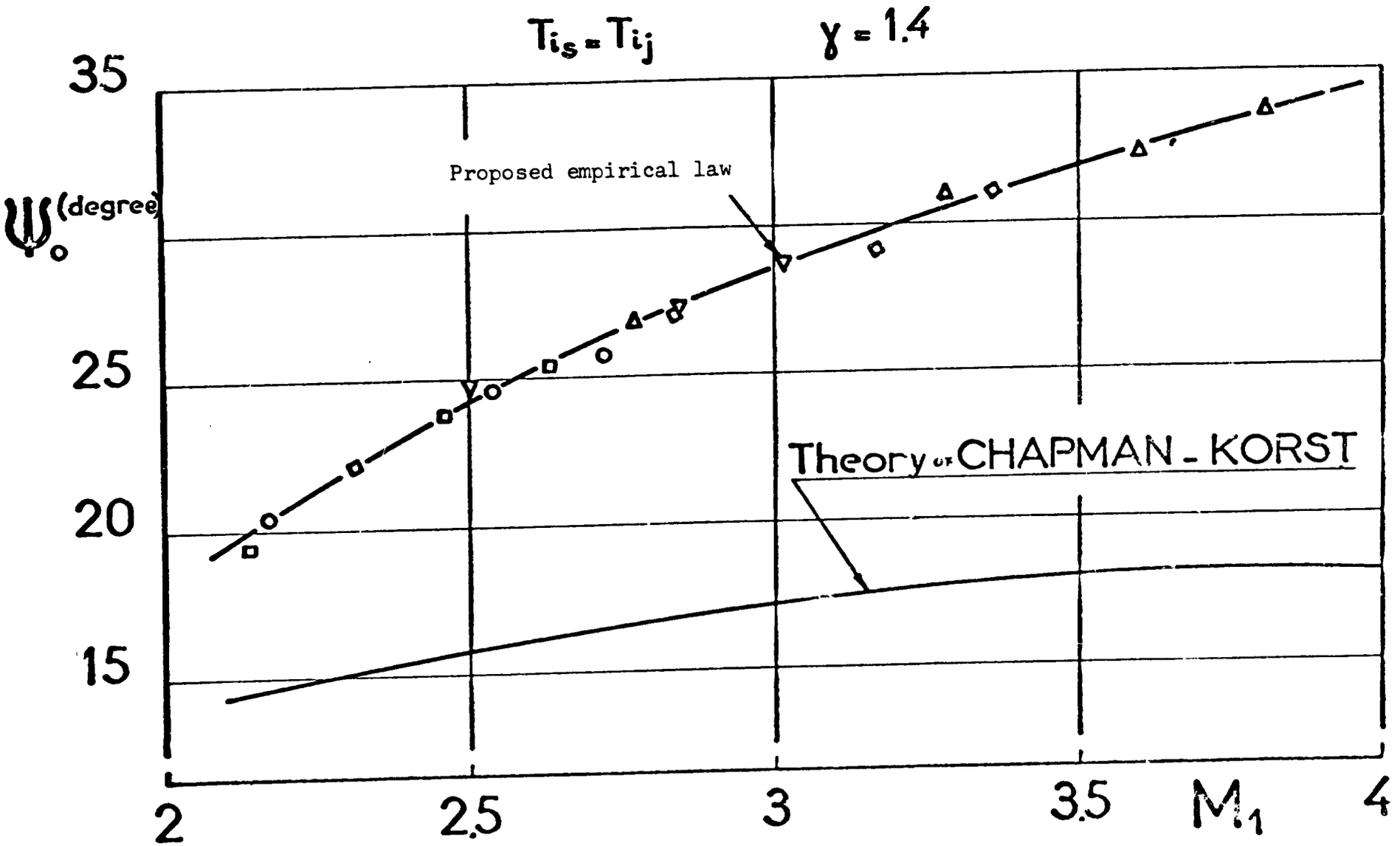

Fig.5 Angular Criterion of Re-Attachment

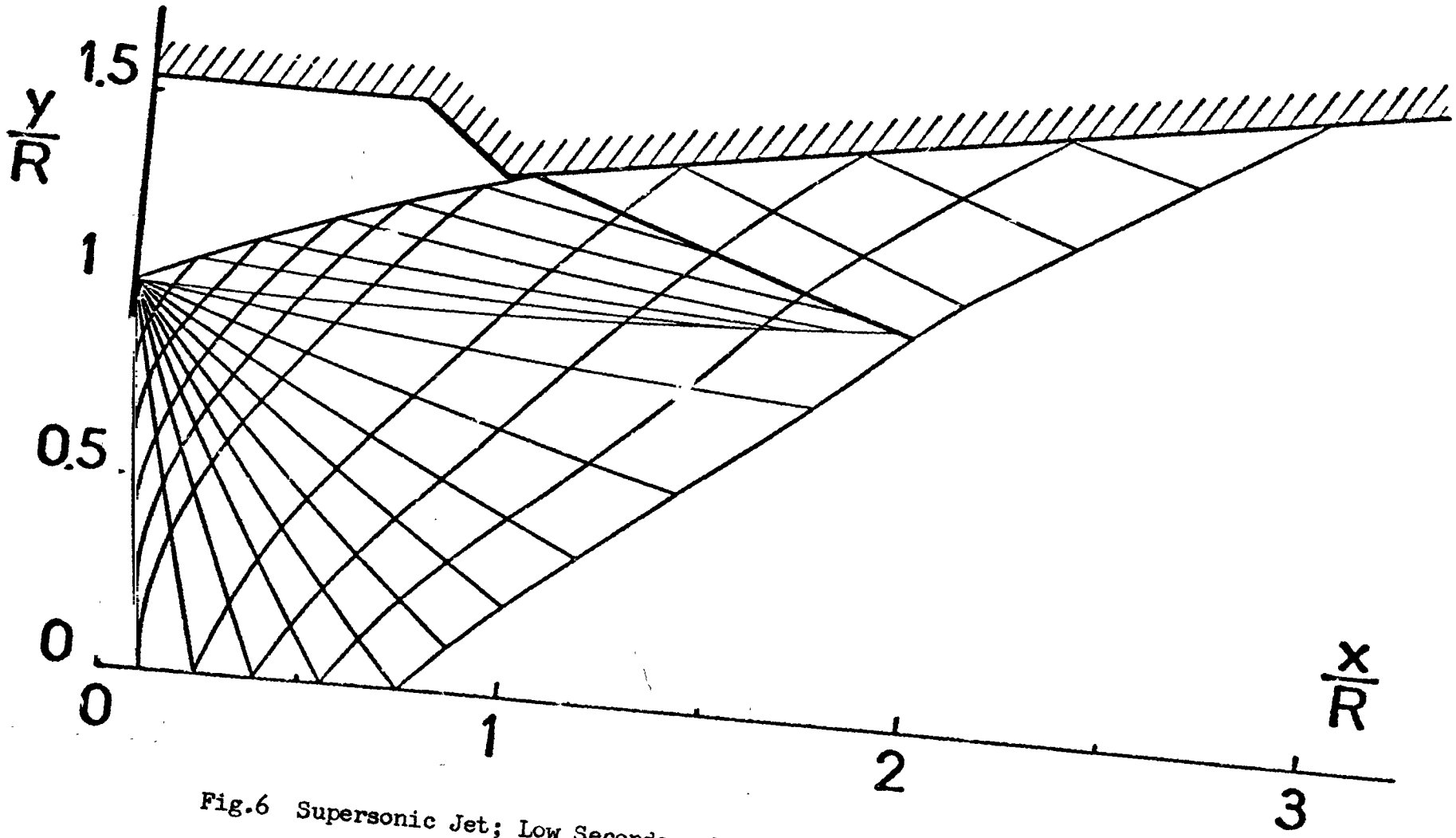

Fig.6 Supersonic Jet; Low Secondary Mass Rate of Flow (μ = 0.005)

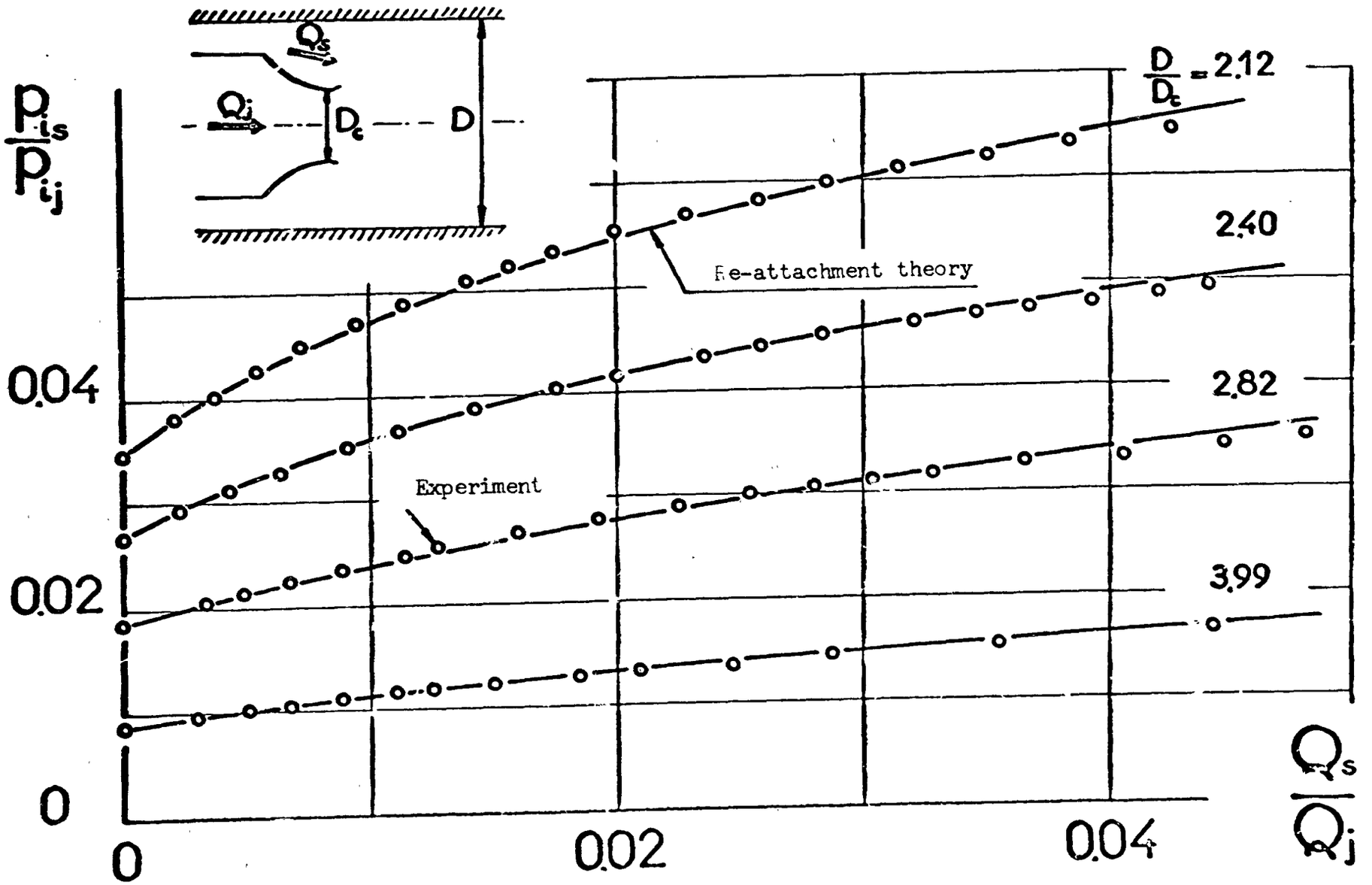

Fig.7 Discharge Performance

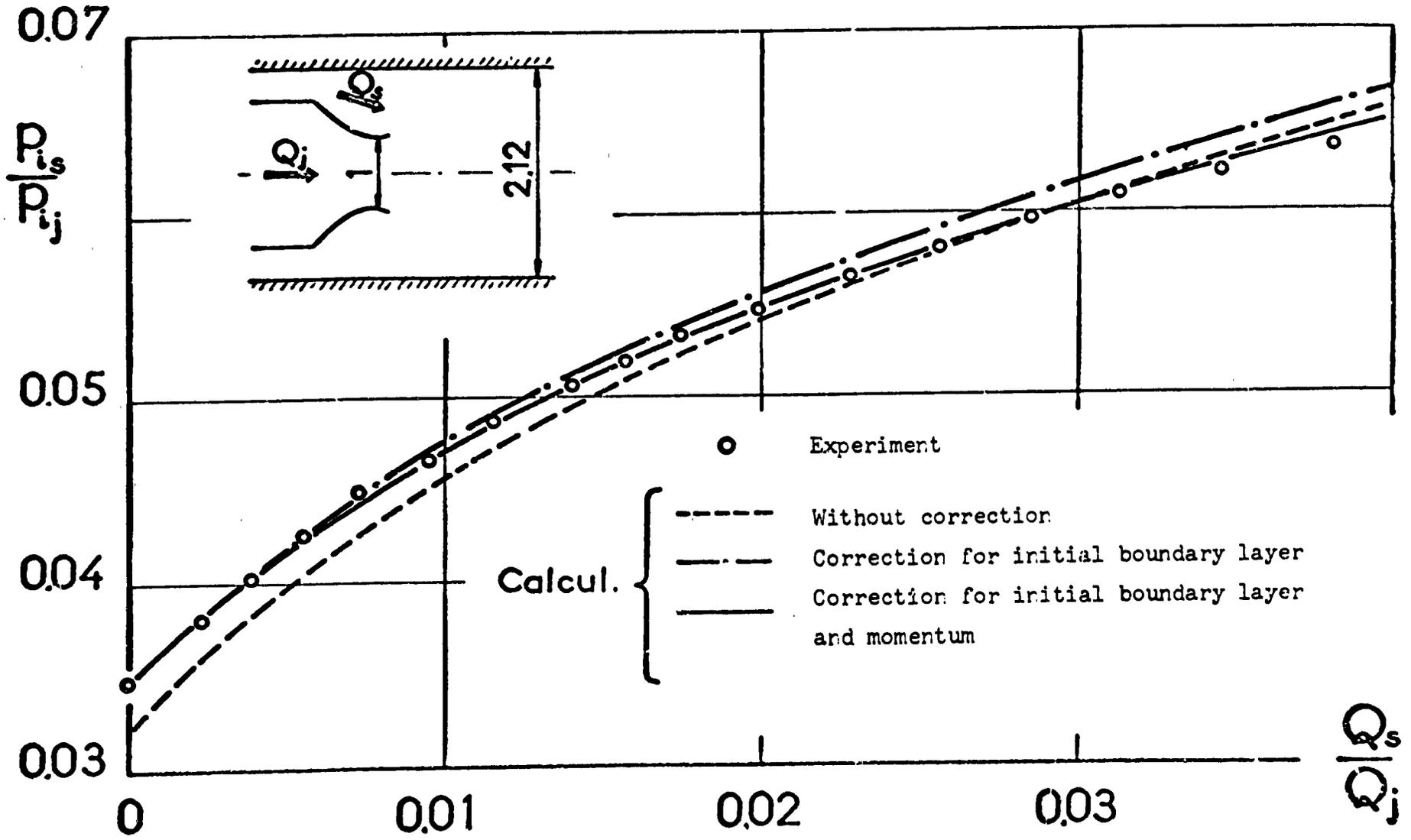

Fig.8 Effects of the Boundary Layer and Momentum

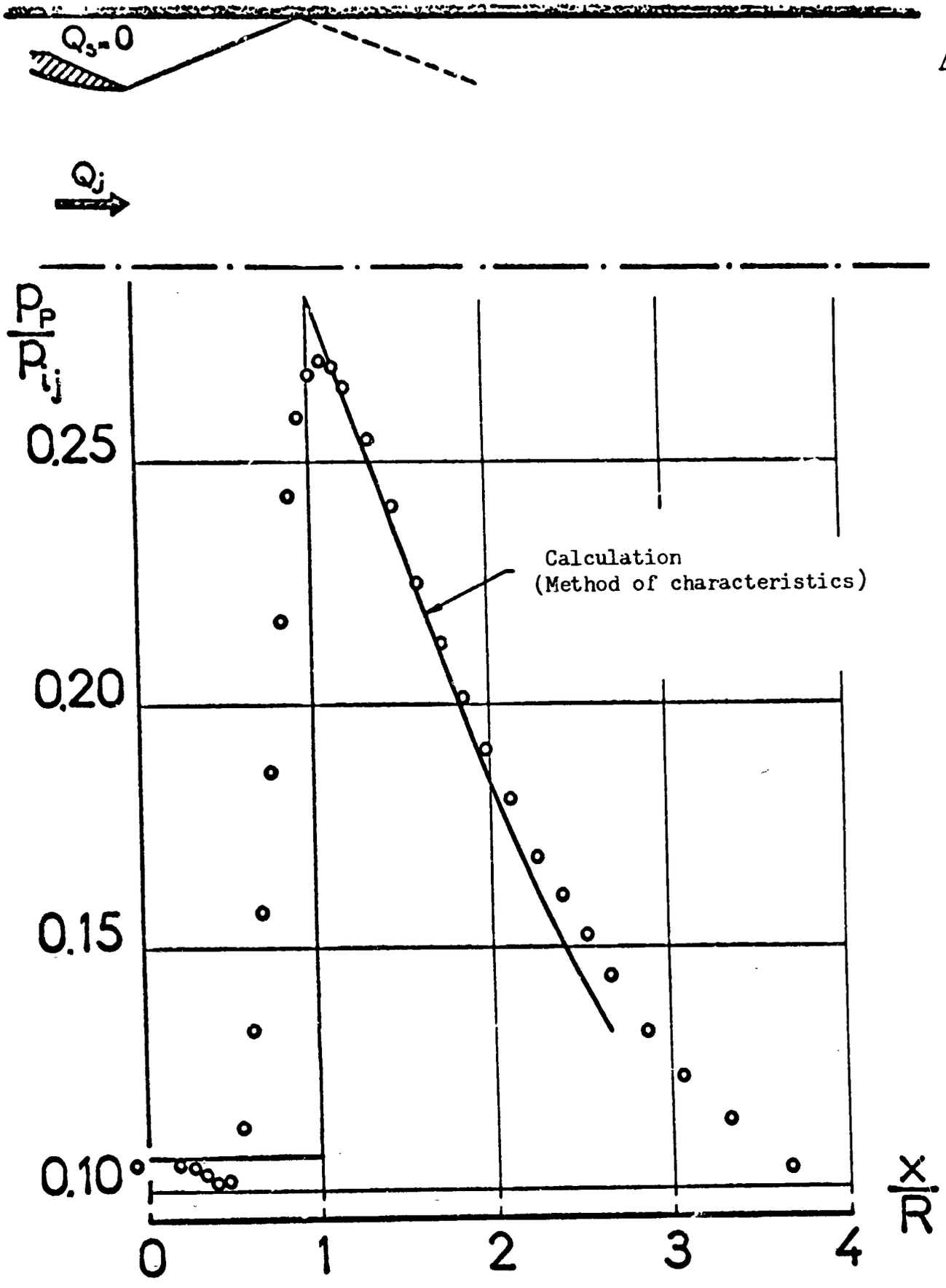

Fig.9 Pressures along the Wall

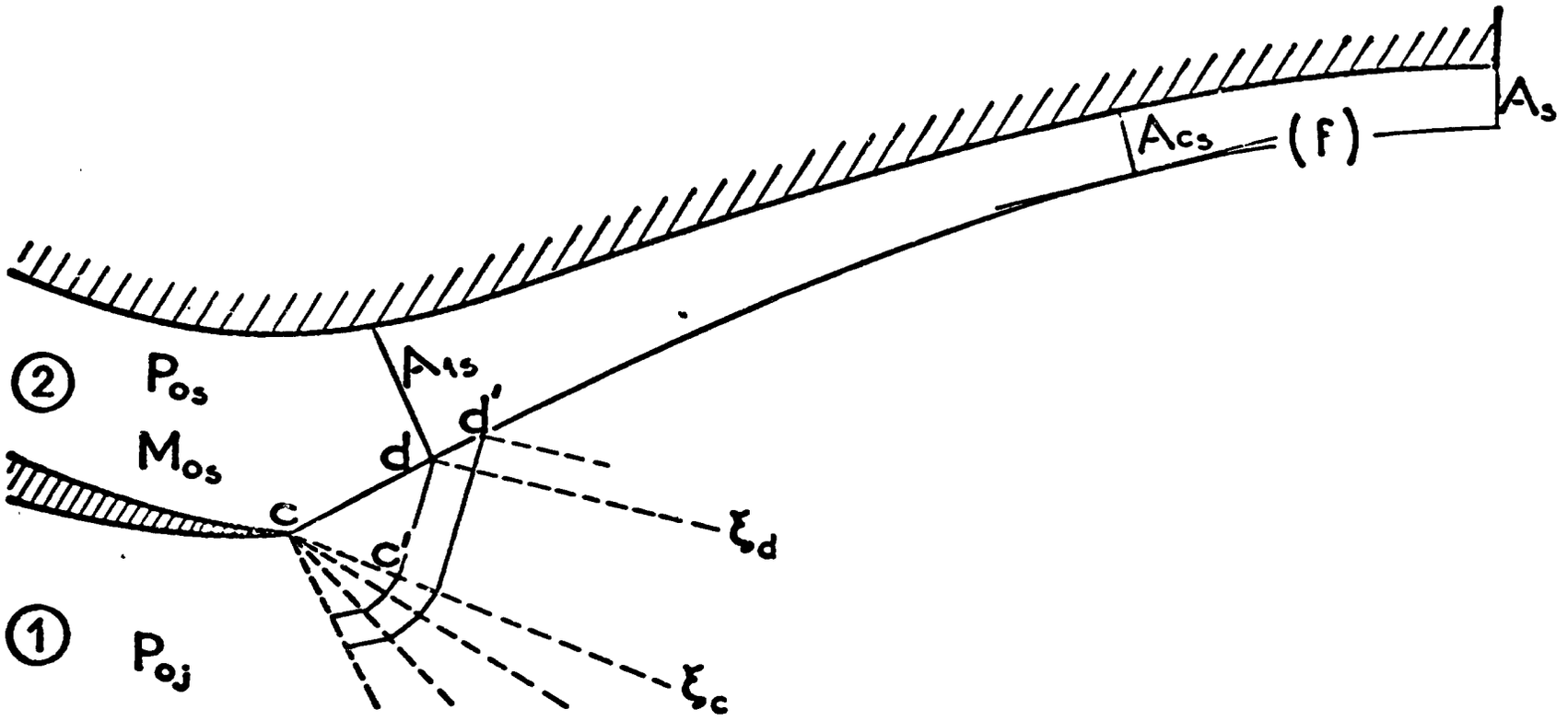

Fig.10 High Secondary Mass Rate of Flow; Computation Scheme

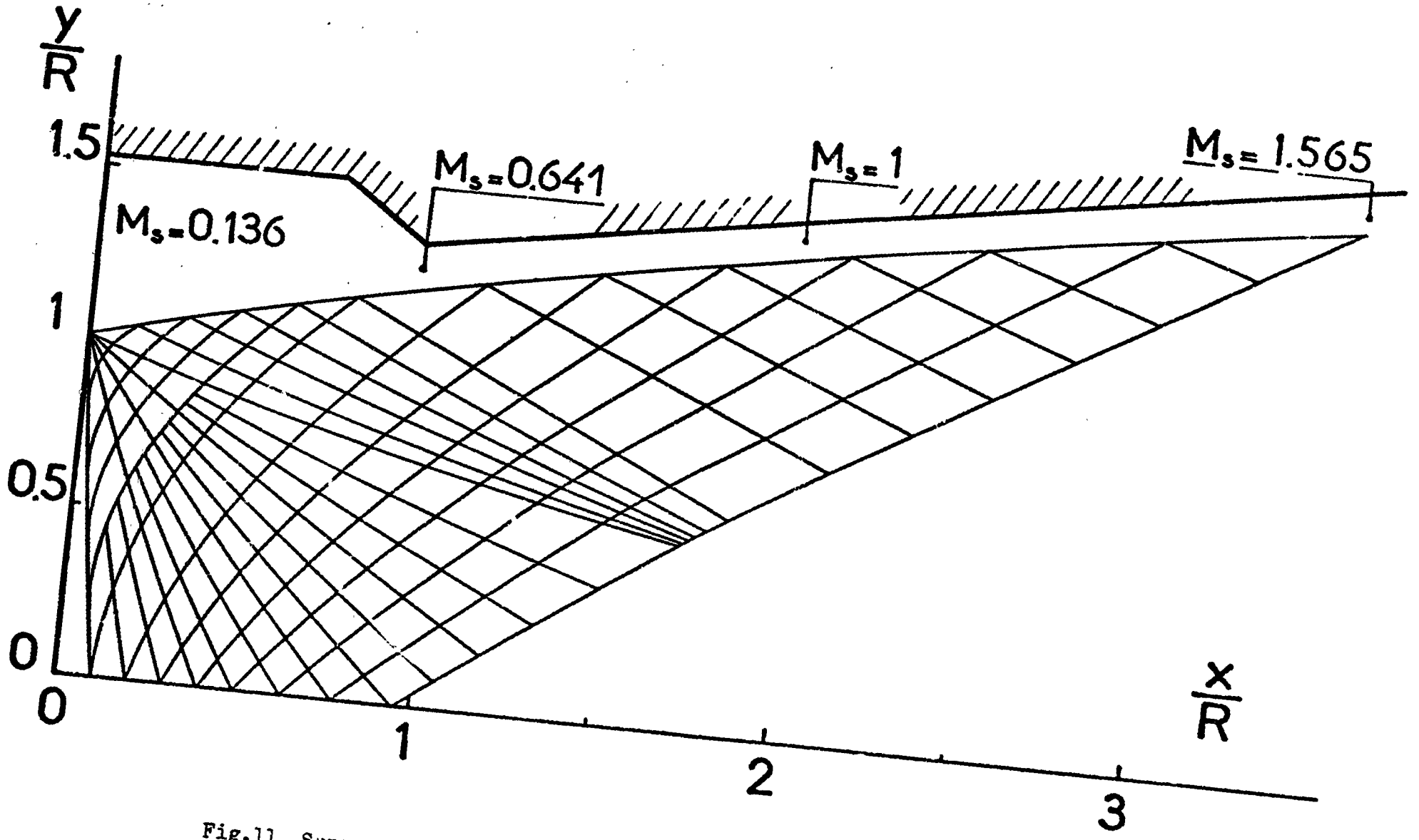

Fig.11 Supersonic Jet; High Secondary Mass Rate of Flow (μ = 0.07)

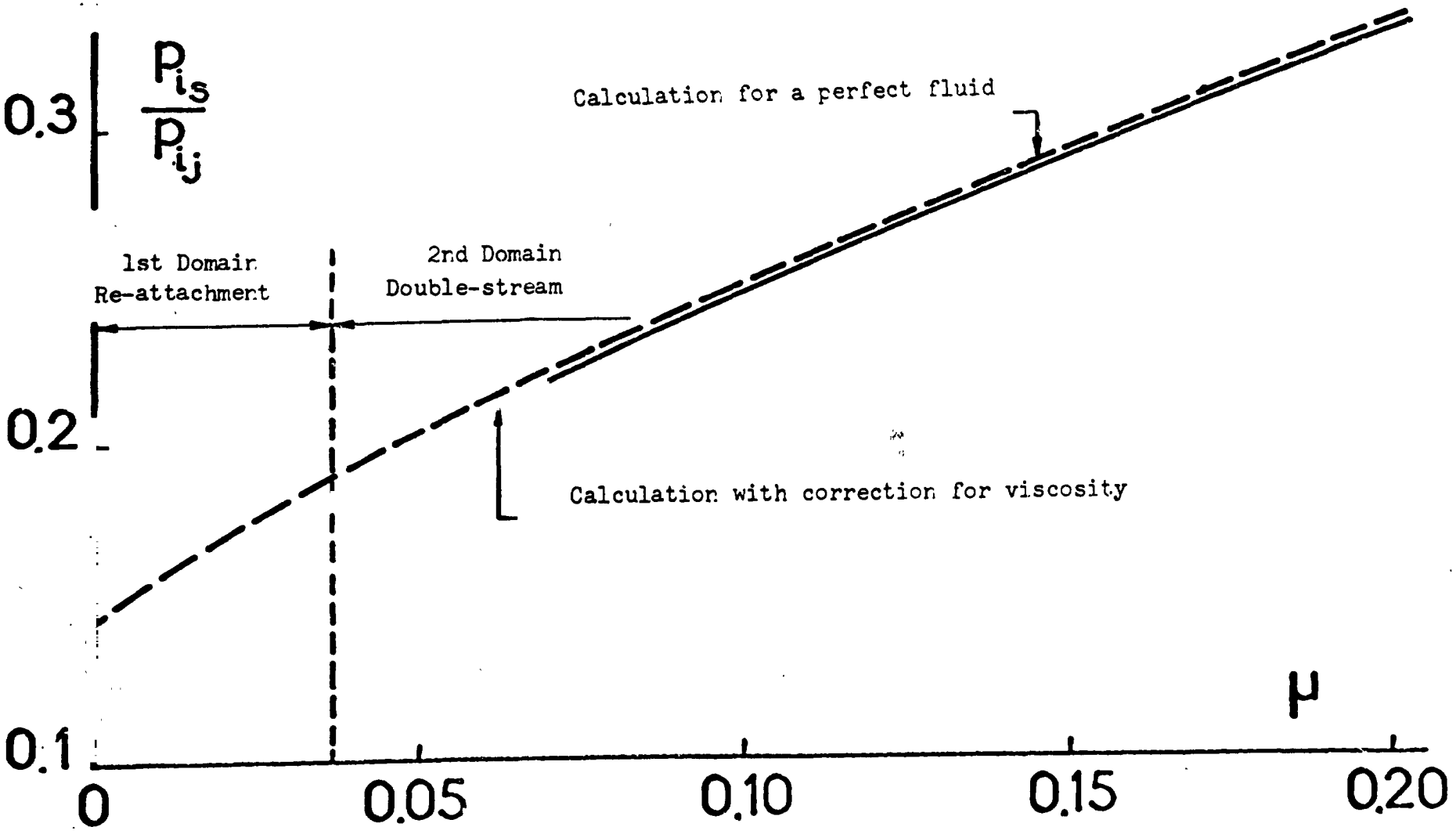

Fig.12 Effect of Entrainment due to Mixing

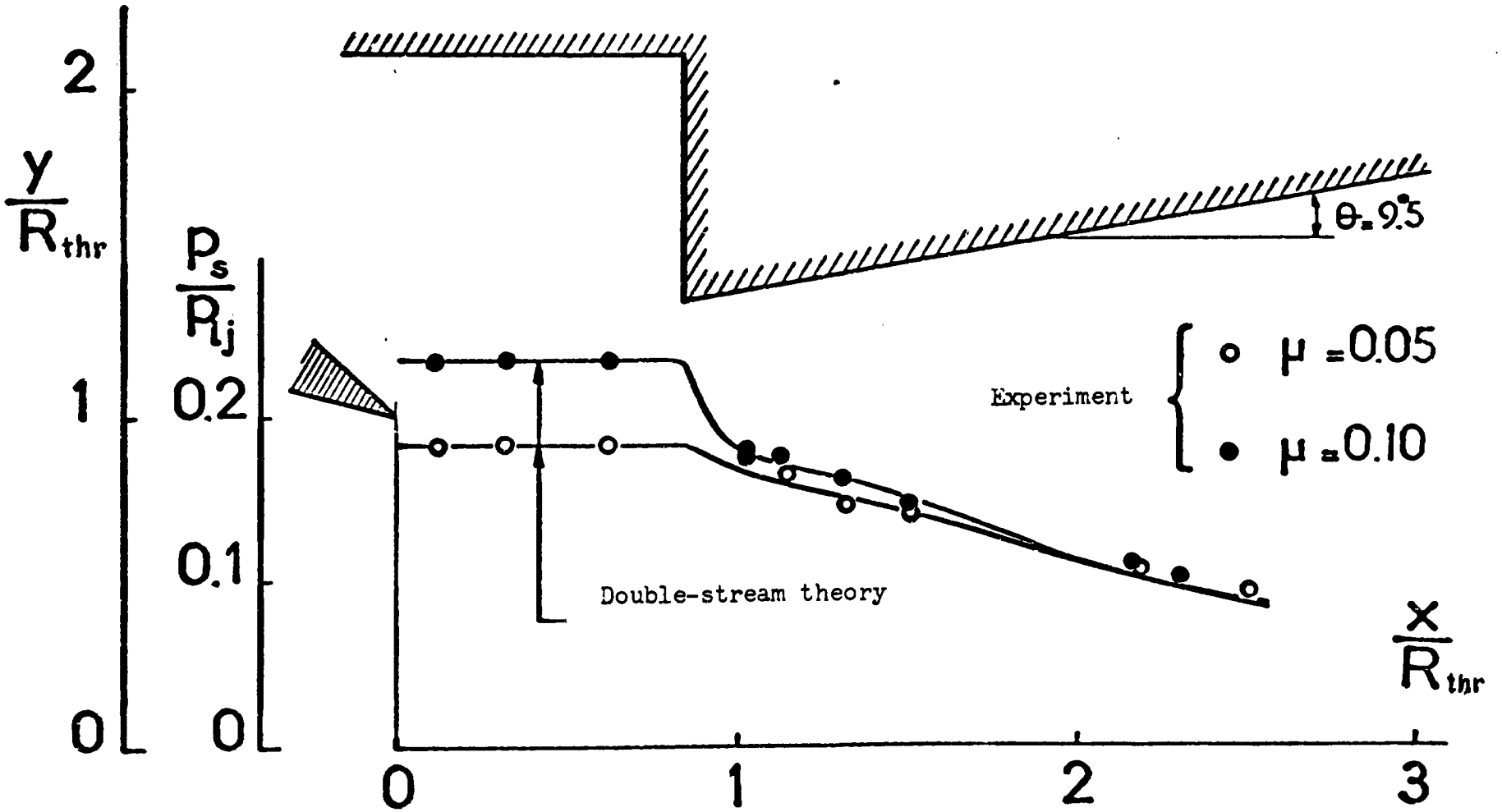

Fig.13 Confrontation of Theory and Experiment; Pressure Distributions

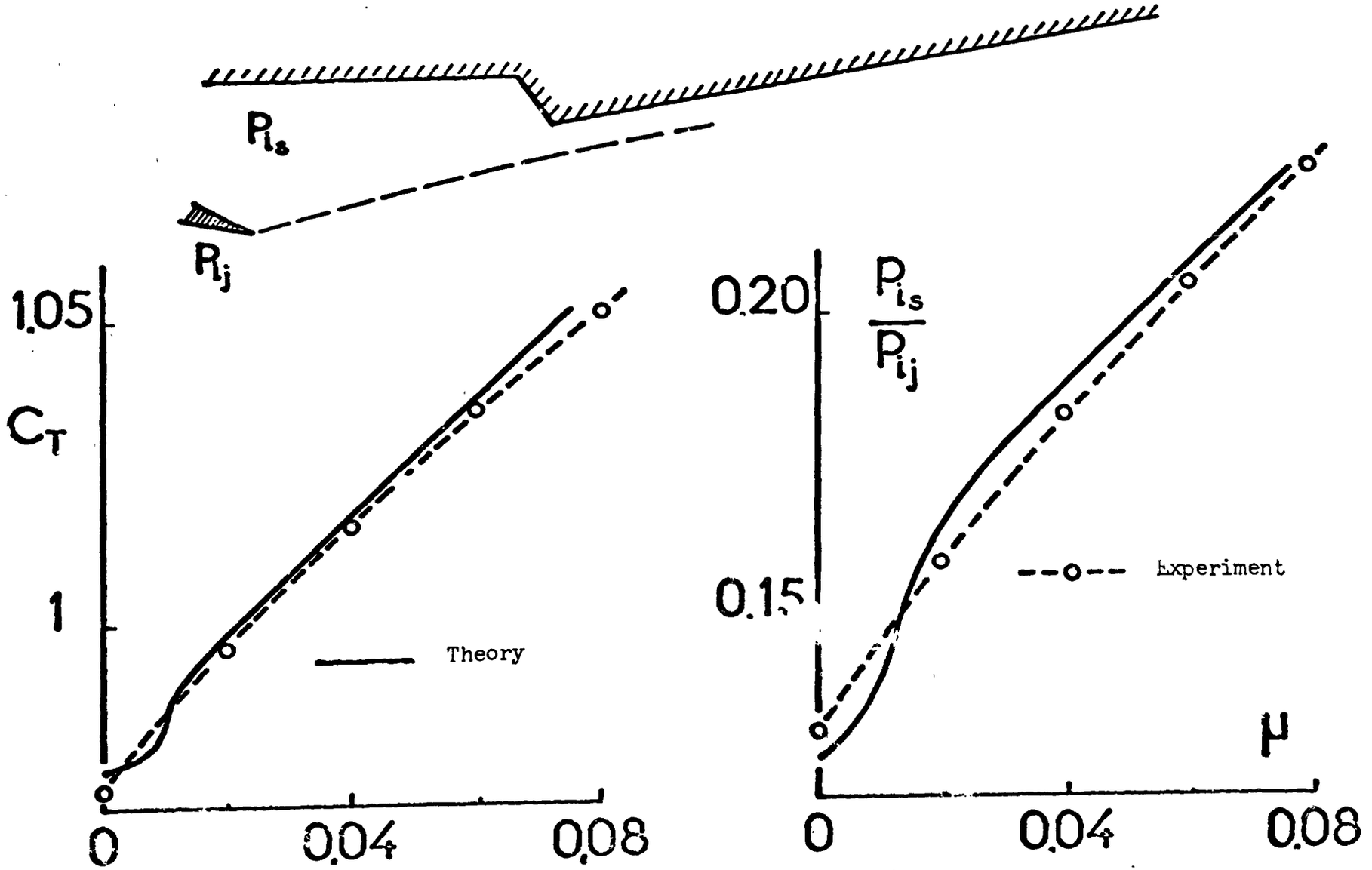

Fig.14a, b Confrontation of Theory and Experiment; Overall Performance

/32

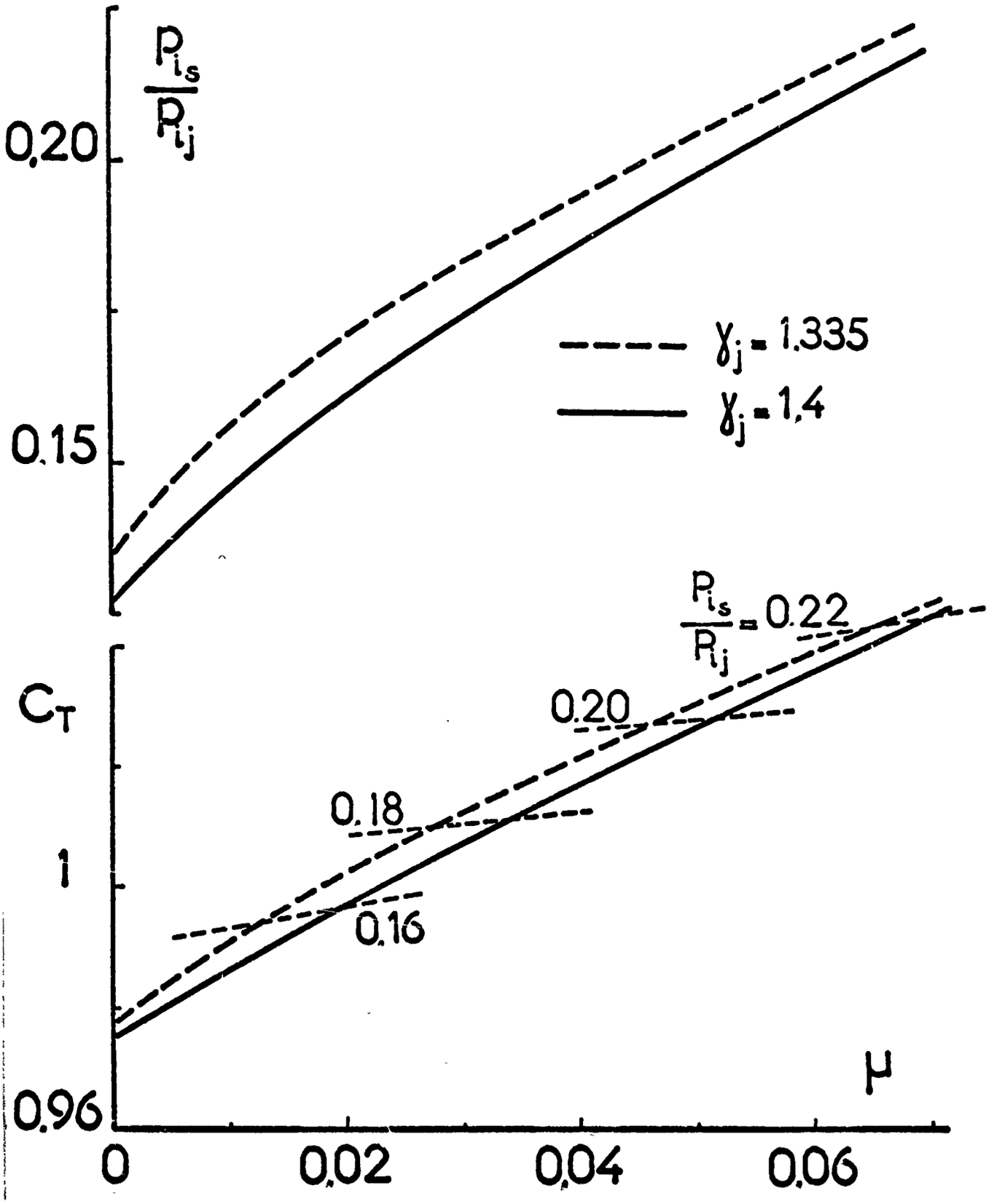

Fig.15 Theoretical Influence of γ